ELSEVIER

Quaternary Science Reviews 24 (2005) 581–594

QSR

Rapid climate change and conditional instability of the glacial deep ocean from the thermobaric effect and geothermal heating

Jess F. Adkins[a,*], Andrew P. Ingersoll[b], Claudia Pasquero[a]

[a] *MS 100-23, Department of Geological and Planetary Sciences, California Institute of Technology, 1200 E. California Blvd., Pasadena, CA 91125, USA*
[b] *MS 150-21, Department of Geological and Planetary Sciences, California Institute of Technology, 1200 E. California Blvd., Pasadena, CA 91125, USA*

Accepted 13 November 2004

Abstract

Previous results from deep-sea pore fluid data demonstrate that the glacial deep ocean was filled with salty, cold water from the South. This salinity stratification of the ocean allows for the possible accumulation of geothermal heat in the deep-sea and could result in a water column with cold fresh water on top of warm salty water and with a corresponding increase in potential energy. For an idealized 4000 dbar two-layer water column, we calculate that there are $\sim 10^6$ J/m^2 ($\sim$0.2 J/kg) of potential energy available when a 0.4 psu salinity contrast is balanced by a $\sim$2 °C temperature difference. This salt-based storage of heat at depth is analogous to Convectively Available Potential Energy (CAPE) in the atmosphere. The "thermobaric effect" in the seawater equation of state can cause this potential energy to be released catastrophically. Because deep ocean stratification was dominated by salinity at the Last Glacial Maximum (LGM), the glacial climate is more sensitive to charging this "thermobaric capacitor" and can plausibly explain many aspects of the record of rapid climate change. Our mechanism could account for the grouping of Dansgaard/Oeschger events into Bond Cycles and for the different patterns of warming observed in ice cores from separate hemispheres.

1. Introduction

One of the most remarkable results of paleoclimate research in the past several decades is the discovery of extremely abrupt, large amplitude climate shifts during the last glacial period, and the contrasting stability of climate during the Holocene (GRIP, 1993; Grootes et al., 1993). First widely recognized as more than climatic "noise" by the drilling of two deep Greenland summit ice cores, these rapid climate changes are organized into several coherent patterns. Twenty-one Dansgaard/Oeschger (D/O) events were originally recognized in the ice cores (Fig. 1) and in the last decade other globally distributed marine records have shown the same pattern of variability (Behl and Kennett, 1996; Charles et al., 1996; Hughen et al., 1996; Schulz et al., 1998). These D/O events are further grouped into packages of "Bond Cycles" (Bond et al., 1993) that are themselves separated by Heinrich events, massive discharges of ice into the North Atlantic (Heinrich, 1988; Hemming, 2004). It is clear that rapid climate changes during the last glacial period were not just bad weather over Greenland but represent a globally coherent pattern of climate instability.

Broecker first proposed that a "salt oscillator" in the Atlantic could drive variability in the ocean's overturning strength and explain these abrupt shifts in climate (Broecker et al., 1990). This idea is based on the modern arrangement of deep-water temperature and salinity. Today the thermohaline circulation is linked to sinking of dense waters in specific regions of the high latitude oceans (Fig. 2). The North Atlantic Ocean around Greenland produces relatively warm and salty North Atlantic Deep Water (NADW) while the Southern Ocean produces relatively cold and fresh Antarctic Bottom Water (AABW). In addition, the δ^{13}C's of

*Corresponding author. Tel.: +1 626 395 8550; fax: +1 626 683 0621.
E-mail address: jess@gps.caltech.edu (J.F. Adkins).

0277-3791/$ - see front matter © 2004 Elsevier Ltd. All rights reserved.
doi:10.1016/j.quascirev.2004.11.005

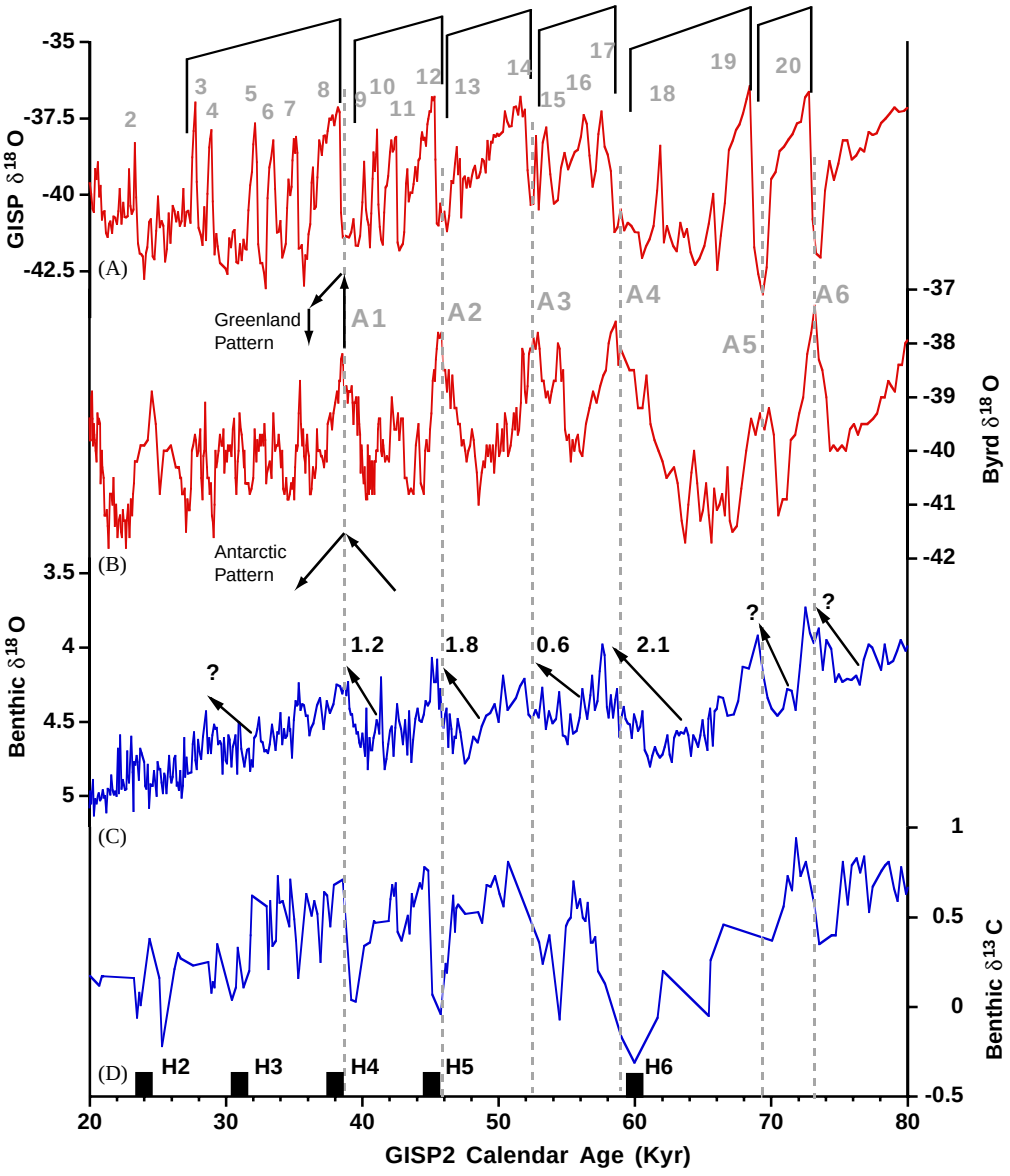

Fig. 1. Ice core and deep ocean records of climate change during the last glacial period. (A) Oxygen isotope variation of the GISP2 ice core on the Blunier and Brook timescale (Blunier and Brook, 2001). $\delta^{18}O$ is a proxy for atmospheric temperature above the ice core (~3000 m altitude). Gray numbers are the interstadial Dansgaard/Oeschger (D/O) warm events. They are grouped into "Bond Cycles" between Heinrich Events (Bond et al., 1993). (B) Same as for 1A but from the Antarctic Byrd ice core. Gray numbers are the Southern Hemisphere events that correspond to the larger D/O events in the north. (C) Benthic foraminifera record of deep ocean temperature and ice volume from 3500 m off of Portugal (core MD95-2042, Shackleton et al., 2000). Lower values represent warming and/or continental ice sheet melting. Black numbers are degrees centigrade of residual $\delta^{18}O$ warming after subtracting the sea level signal from New Guinea coral reef profiles (Chappell, 2002). Question marks are possible deep temperature increases that are not covered by the Huon record. The black arrows show the sense of temperature rise but they are not meant to imply we know the timing of deep ocean warming. (D) Benthic $\delta^{13}C$ from the same core as in 1C. Black bars at the bottom of the figure correspond to the ages of Heinrich Events as determined by Hemming (2004). Errors in the calendar age estimates of all climate events in this figure increase with increasing age. The errors in the ages of Heinrich events H3-H5 are probably larger than the width of the black bars. Slight differences in phasing between ice core warmings, Heinrich events and the benthic isotope records are not robust given the calendar age uncertainties.

newly formed NADW and AABW are about 1.1‰ and 0.5‰ respectively. Fig. 2a shows the imprint of the overturning circulation on the $\delta^{13}C$ of dissolved inorganic carbon in the modern ocean. Relatively enriched $\delta^{13}C$ water from the north fills much of the modern deep Atlantic. As it is denser than the NADW, isotopically depleted AABW occupies the abyss. In Broecker's salt oscillator idea, the glacial overturning circulation is similar to the modern arrangement except that fresher waters in the high latitude North Atlantic surface cause a reduction in NADW flux and a corresponding increase in the volume of Southern source waters in the Atlantic. A simple model of the coupled glacial ocean and atmosphere, which still has

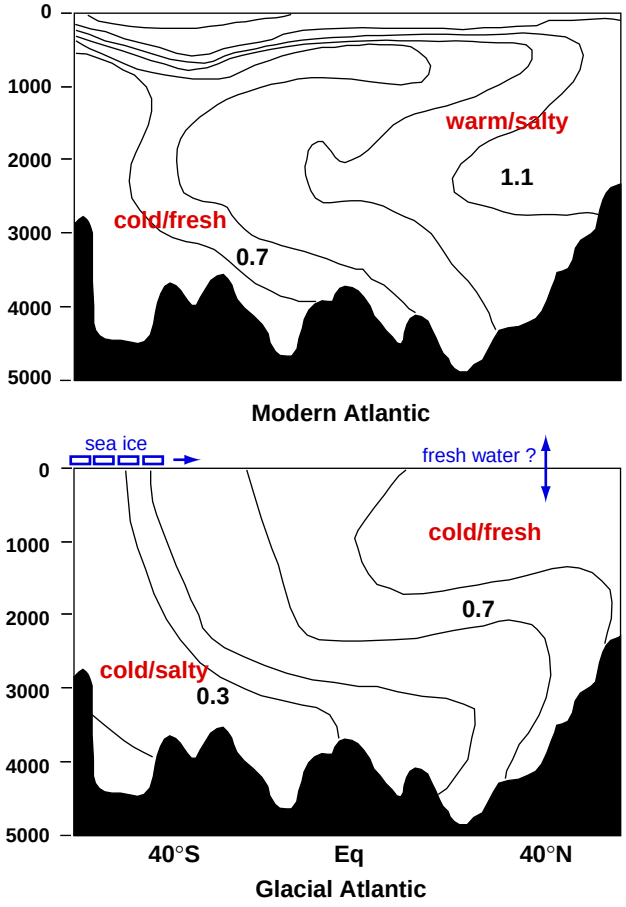

Fig. 2. Schematic of the modern and glacial arrangement of deep waters in the Atlantic Ocean after Labeyrie et al. (1992). Black isolines are the $\delta^{13}C$ of dissolved inorganic carbon (Modern case) and of benthic foraminifera (LGM case). They show an increased volume of Southern source waters, at the expense of Northern source waters, during the glacial. The relative temperature and salinity of each water mass are shown in red. At the LGM, southern source waters were about 0.4 psu saltier than the rest of the Atlantic and make it difficult for fresh water forcing at the northern source to alter the overturning circulation. The cause of the southern saltiness is shown schematically by sea ice export out of the regions around Antarctica.

higher salinity in the north, also shows abrupt climate changes that are associated with rapid switches in the strength of the overturning circulation and that look similar to the Greenland ice core record (Ganopolski and Rahmstorf, 2001). In this model, imposed glacial boundary conditions at the surface of the ocean cause the stability diagram of the overturning circulation to become more sensitive to fresh water forcing in the high latitude North Atlantic. Small changes in the salt flux at these high latitudes cause the overturning circulation to flip between northern and southern source dominated sinking in the Atlantic.

However, the LGM deep circulation in the Atlantic does not look like the modern circulation with an added sensitivity to fresh water forcing. From the distribution of $\delta^{13}C$ in benthic foraminifera we know that Southern source waters filled the basin in the past (Duplessy et al., 1988). By themselves these passive tracer data can be consistent with a salt oscillator causing northern source waters to become fresher and therefore less dense. This increased buoyancy in the north could then allow cold and fresh southern source waters to fill the Atlantic. However, the reconstruction of LGM temperature and salinity from deep-sea pore fluids shows that the modern arrangement of salty northern source waters and relatively fresh AABW was reversed during the glacial (Adkins et al., 2002). A plausible mechanism for increasing the salinity of the sinking Southern Ocean water is to increase the sea ice export out of the deep-water formation regions around Antarctica (Keeling and Stephens, 2001). In fact, the water $\delta^{18}O$ and salinity data from the pore fluids confirm this hypothesis and constrain the northern source waters to be about 0.4 psu fresher than the southern source waters. Overall, this salty southern sinking leads to increased deep stratification in the glacial Atlantic, as compared to today, and it changes the sensitivity of the overturning circulation to fresh water forcing at the northern surface. During the glacial, the density of the deepest waters, which are nearly frozen and are the saltiest waters in the ocean, must be reduced before salt forcing at the surface can reinvigorate the North Atlantic overturning. Some other mechanism must first change the salt dominated stratification of the deep Atlantic before fresh water forcing of northern source waters can induce "flips" in the overturning circulation. If the LGM temperature and salinity distribution is characteristic of the glacial period in general, then "salt oscillator" mechanisms need help to change the deep circulation pattern.

The solar energy flux of $\sim 200\,W/m^2$ at the ocean's surface (Peixoto and Oort, 1992) is much larger than the next largest potential source of energy to drive climate changes, geothermal heating at the ocean's bottom ($50–100\,mW/m^2$) (Stein and Stein, 1992), but this smaller heat input might still play an important role in rapid climate changes. It is clear that variations in the solar flux pace the timing of glacial cycles (Hays et al., 1976), but these Milankovitch time scales are too long to explain the decadal transitions found in the ice cores. Another, higher frequency, source of solar variability that would directly drive the observed climate shifts has yet to be demonstrated. Therefore, mechanisms to explain the abrupt shifts all require the climate system to store potential energy that can be catastrophically released during glacial times, but not during interglacials (Stocker and Johnsen, 2003). At the Last Glacial Maximum (LGM), when the deep ocean was filled with salty water from the Southern Ocean, geothermal heating may have been an important source of this potential energy. While Southern Ocean deep-water formation resulted in a deep ocean filled with cold salty waters from the south, northern source overturning was

still active at the LGM (Boyle and Keigwin, 1987) but it was fresher by at least 0.4 psu and less dense by comparison (Adkins et al., 2002). Both water masses were at or near the freezing point of seawater with slightly colder northern source waters sitting on top of southern source waters (Fig. 2b). In light of this salinity control of density contrasts, as opposed to the modern largely thermal stratification, geothermal heating can lead to "trapped" heat in the glacial deep ocean. This geothermal heat could provide the density decrease needed in the deep Atlantic to make the system become sensitive to changes in the fresh water budget at the surface. In addition, the seawater equation of state, through "thermobaricity", allows for geothermal heat to be stored and catastrophically released in a system with cold fresh waters on top of warm salty waters.

In modern ocean studies there is an increasing awareness of the effect of geothermal heating on the overturning circulation. As an alternative to solar forcing, Huang (1999) has recently pointed out that geothermal heat, while small in magnitude, can still be important for the modern overturning circulation because it warms the bottom of the ocean, not the top. Density gradients at the surface of the ocean are not able to drive a deep circulation without the additional input of mechanical energy to push isopycnals into the abyss (Wunsch and Ferrari, 2004). Heating from below, on the other hand, increases the buoyancy of the deepest waters and can lead to large scale overturning of the ocean without additional energy inputs. Several modern ocean general circulation models have explored the overturning circulation's sensitivity to this geothermal input. In the MIT model a uniform heating of 50 mW/m^2 at the ocean bottom leads to a 25% increase in AABW overturning strength and heats the Pacific by ~0.5 °C (Adcroft et al., 2001; Scott et al., 2001). In the ORCA model, applying a more realistic bottom boundary condition that follows the spatial distribution of heat input from Stein and Stein (1992) gives similar results (Dutay et al., 2004). In both models, most of the geothermal heat radiates to the atmosphere in the Southern Ocean, as this is the area where most of the world's abyssal isopycnals intersect the surface.

In this paper we explore the possibility that during the last glacial period geothermal heating may have been even more important than it is today to the overturning circulation. Continually warming waters stored below a cold layer will eventually lead to an unstable situation. However, even before this critical point is reached, thermobaricity in the seawater equation of state can trigger ocean overturning in an otherwise statically stable water column. Warm waters below cold waters can be stable relative to small vertical perturbations but unstable to larger movements, due to the "thermobaric effect". After deriving an expression that is analogous to CAPE in the atmosphere, we will demonstrate the potential for this abrupt energy release and we will discuss its relation to the record of rapid climate changes in the past.

2. The thermobaric effect and our calculation method

Thermobaricity is the coupled dependence of seawater density on pressure and temperature (Mcdougall, 1987). The first derivative of seawater density with temperature is the thermal expansion coefficient, alpha (α). Alpha itself is both temperature and pressure dependent (as shown in Fig. 3), leading to "cabbeling" and "thermobaricity", respectively. At constant pressure α increases with increasing temperature. The resulting curved isopycnals in a temperature/salinity (T/S) plot imply that waters of the same density, but different combinations of T and S, will always form a more dense fluid when mixed together, giving rise to "cabbeling". Similarly, α increases with increasing pressure. This thermobaric effect means that temperature differences between waters have a larger effect on density differences when the waters are deep than when the waters are shallow. In a statically stable system where cold/fresh water is on top of warm/salty water (Fig. 4), cooler waters from the surface will be denser than the warmer waters below if they are pushed to a depth where the effect of lower temperature on density overcomes the effect of lower salinity (transition from Fig. 4a to b). Even in a statically stable water column, water pushed below this "critical depth" (known as the level of free

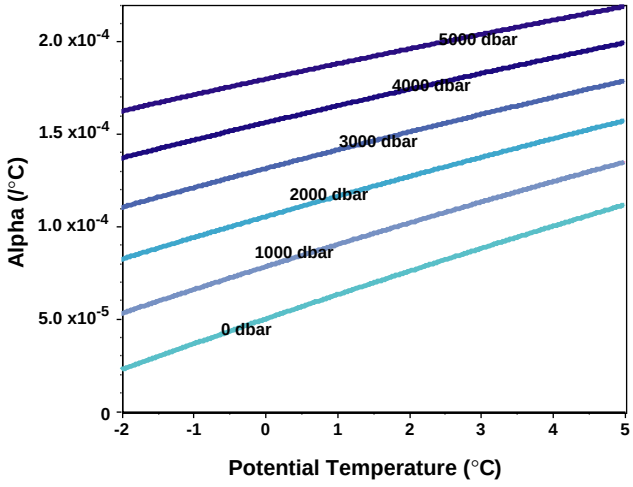

Fig. 3. The pressure and temperature dependence of alpha, the thermal expansion coefficient of seawater. The sensitivity of density to changes in temperature is itself temperature dependent ("cabbelling") and leads to curved isopycnals in plots of temperature versus salinity. This temperature sensitivity is also pressure dependent such that waters at higher pressure have larger density changes for a given temperature change. This effect is itself temperature dependent as the isolines are closer together at higher temperatures than they are at cooler ones.

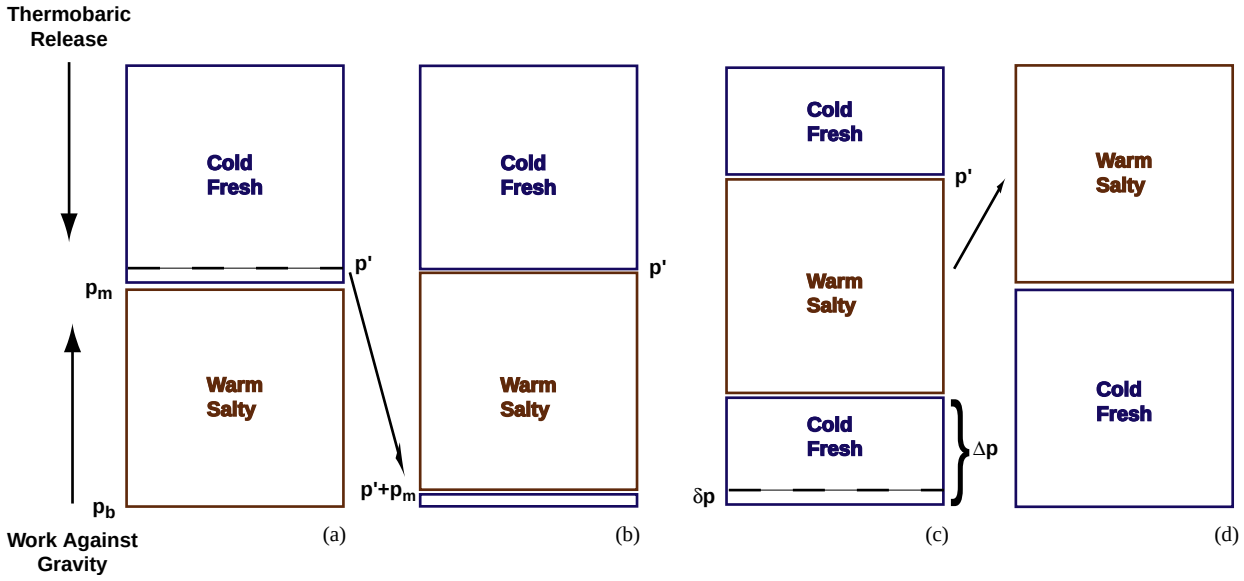

Fig. 4. Scheme for calculating the potential energy contained in a two-layer system of warm, salty water below cold, fresh water. For certain choices of T and S, moving a single layer from the top water mass to the bottom of the column will lower the overall potential energy of the system (transition from (a) to (b)). If many layers are moved then the total energy change for a thickness Δp can also be calculated (c). A complete flip-flop of the two layers (d) will nearly balance the thermobaric release of energy with the work required to lift the warm, salty layer. See text for details. Δp and δp are discussed in the appendix.

convection) can cause the system to overturn. A system with warm/salty water below cold/fresh water holds the upper layer higher above the geoid than if some of the cold water were moved to the bottom.

This thermobaric effect is a potential energy storage mechanism, a capacitor, which can result in an abrupt overturn of the water column. Its relevance has been recognized in the formation of the convective chimneys of the modern Weddell Sea (Killworth, 1979; Akitomo, 1999a) and in setting the depth of convection in the Greenland Sea (Denbo and Skyllingstad, 1996). To simplify the arguments and calculate the energy available from thermobaric instability in a salt stratified ocean, we consider a water column composed of two layers of equal mass but different temperature and salinity. We measure pressure relative to atmospheric pressure, so the surface pressure is zero and the bottom pressure is p_b. Initially the top layer occupies the pressure range $0<p<p_m=p_b/2$ and is colder and fresher than the bottom layer, which occupies the pressure range $p_m<p<p_b$ (see Fig. 4a). Ingersoll (2005) considered the same system using a simplified equation of state. Within each layer potential temperature and salinity are homogeneous, while density varies with depth according to the pressure dependence in the seawater equation of state. We move parcels from the base of the top layer (p') to the base of the bottom layer ($p'+p_m$). The first parcel is moved from its initial pressure $p'=p_m$ to p_b. As more parcels are moved, p' decreases (Figs. 4b and c). In general, the energy per unit mass released by adiabatically moving a parcel from pressure p' to pressure $p'+p_m$ (analogous to CAPE in a moist atmosphere) is (Fig. 4b):

$$\frac{\text{Energy}}{\text{mass}}=\int_{p'}^{p'+p_m}(V_{\text{fluid}}-V_{\text{parcel}})\,dp, \tag{1}$$

where $V_{parcel}(p)$ and $V_{fluid}(p)$ are the specific volume of the parcel and of the ambient fluid, respectively, calculated at the pressure level p, and assuming that potential temperature and salinity are conserved during vertical displacements (see the appendix for a derivation of the equations in this section under more general conditions). The full seawater equation of state (Fofonoff, 1985) is used to calculate the specific volumes so that the thermobaric terms are included in the overall energy balance. Potential energy can be released any time that the final pressure of the top water parcel is moved below the Level of Free Convection, defined as the pressure at which $V_{parcel}(p)=V_{fluid}(p)$ (see Fig. 6). When a group of water parcels of thickness Δp is moved from the top layer to the base of the bottom layer, which is correspondingly displaced upwards, the released energy (per unit mass of the whole system) is (Fig. 4c):

$$\frac{\text{Total energy}}{\text{mass}}=\frac{-1}{p_b}\int_{p_m}^{p_m-\Delta p}\left[\int_{p'}^{p'+p_m}(V_{\text{fluid}}-V_{\text{parcel}})\,dp\right]dp'. \tag{2}$$

The complete switch between the two water masses corresponds to $\Delta p=p_m$ (Fig. 4d).

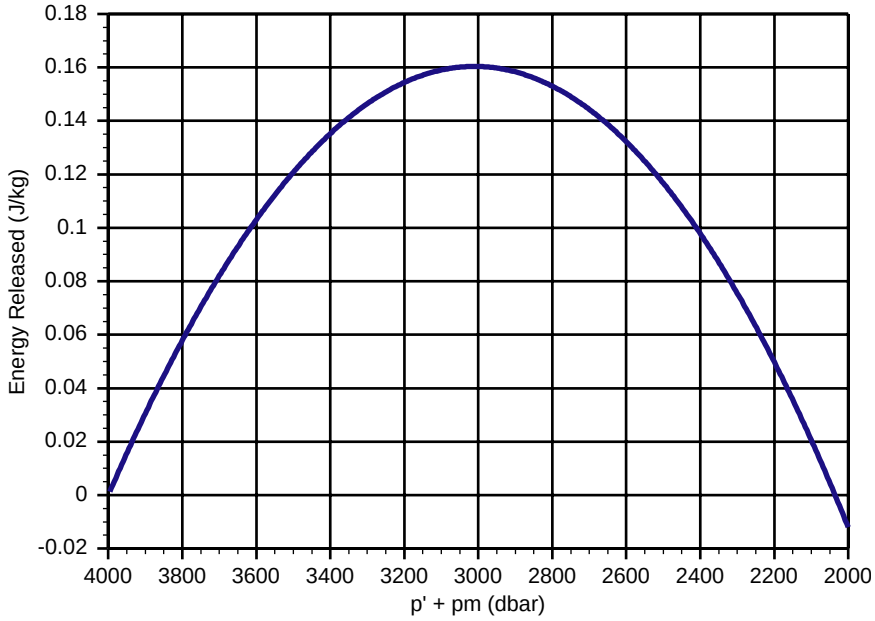

Fig. 5. Energy released from pushing cold/fresh water below warm/salty water in the two-layer system shown in Fig. 4. Two 2000 dbar thick layers were used in this calculation; top layer $\Theta = 0\,^{\circ}C$ and salinity = 34.7 psu, bottom layer $\Theta = 2.4884$ and salinity = 35.0 psu. This arrangement assures neutral stability at the 2000 dbar layer interface. Successive 0.4 dbar thick layers were moved to the bottom of the water column and the final minus initial energy was calculated. The integrated energy released has a maximum at 1000 dbars moved to the bottom and nearly all total thicknesses moved will release energy. A complete "flip-flop" of the two layers is almost energy neutral (see text).

3. Results

By changing the value of Δp between 0 and p_m, we can find the water column configuration corresponding to the maximum energy release. Fig. 5 shows the result of this calculation for a 4000 dbar water column with the top water mass potential temperature (θ) and S equal to $0\,^{\circ}C$ and 34.7 psu respectively, and with bottom water values of $2.4884\,^{\circ}C$ and 35.1 psu, respectively. The values have been chosen to ensure that the in situ density difference at $p = p_m$ is zero, such that the static stability of the water column is neutral, and to match the measured LGM salinity gradient between southern and northern source waters. Energy release is at a maximum of 0.16 J/kg for about one-half of the top layer being pushed to the bottom. Total exchange of the two water masses is almost energy neutral (right hand side of Fig. 5). A slight energy input into the system is needed to achieve this complete exchange because the increase of α with pressure is itself temperature dependent (Fig. 3). The cold water mass experiences a slightly larger change in α than the warmer water mass leading to the imbalance at the complete exchange state. Our maximum energy of 0.16 J/kg for a temperature difference of $2.4884\,^{\circ}C$ compares well with the idealized equation of state computation in Ingersoll (2005) who found 0.3 J/kg for a temperature difference of $4\,^{\circ}C$.

Our calculation method demonstrates that a warm/salty water mass underneath a cold/fresh water mass, with a neutrally stable interface, can contain potential energy. The next question is, "how might this energy be released?" To investigate this problem we consider the same water mass arrangement as in Fig. 4 but now with the bottom water θ as a variable and the salinities the same as before. Starting with θs that are warmer than the top box but not at the point of neutral stability, we calculate the maximum energy released (apex of Fig. 5) for a continual warming of the bottom water to the point where "normal" convection would occur. Beginning with a bottom θ value of $1.8\,^{\circ}C$, the water mass interface is very stable (Fig. 6a). For this θ, forcing layers of water from the cold top water to the bottom of the column requires net energy input to the system over the whole range of Δp values (Fig. 6b). However, at a bottom water θ of about $2.1\,^{\circ}C$ the first layer moved from the top to the bottom releases a small amount of energy. This trend continues as the bottom layer is warmed with more of the cold top layer becoming available to release larger and larger amounts of energy when moved to the bottom (Fig. 6b). When the system warms to the point where the density contrast at p_m favors convection, the water column is poised for a catastrophic overturning. Deep heating has charged a "thermobaric capacitor" (see the curve in Fig. 6b), which once triggered will release potential energy that eventually induces mixing in large portions of the water column (Akitomo, 1999a).

Note that our simple model does not consider mixing and the entropy change associated with it, nor does it allow the released energy to further mix the water

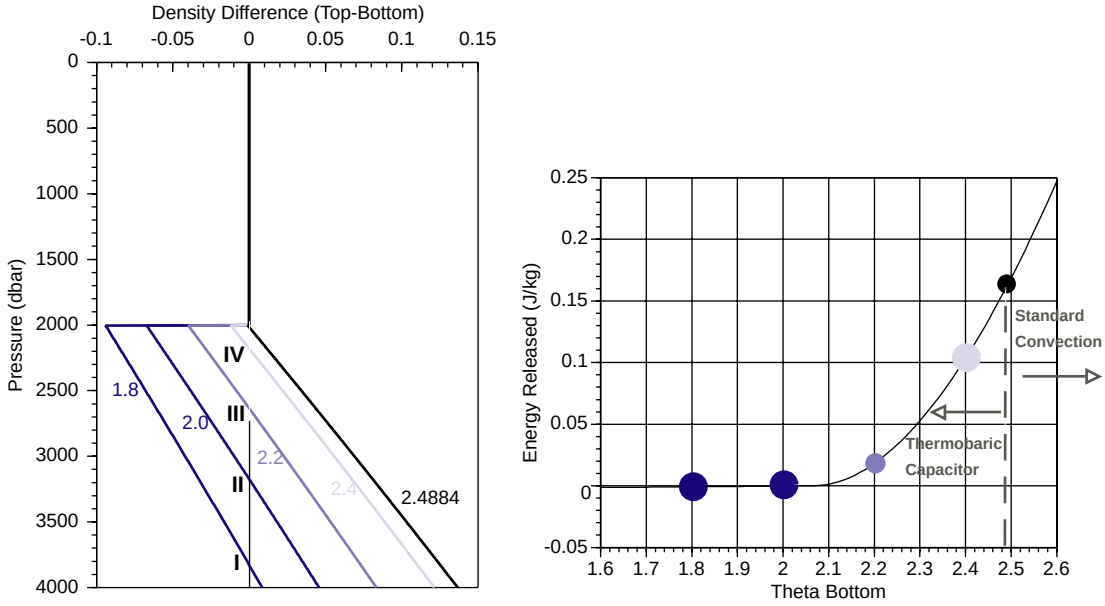

Fig. 6. (a) Density difference between a parcel of water with $\Theta = \Theta_{top} = 0\,^{\circ}C$ and $S = S_{top} = 34.7$ psu and the ambient water in the two-box configuration, as function of pressure. The bottom water has salinity $S = S_{bottom} = 35.1$ psu, and $\Theta = \Theta_{bottom}$ as indicated in the figure. At first, work is required to push the parcel down within the bottom water mass; when the Level of Free Convection (i.e. the pressure at which the density difference is equal to zero, see points I–IV) is reached the parcel becomes statically unstable and freely moves downward releasing potential energy. For points I and II the potential energy released is smaller than the energy needed to push the parcel from the layer interface to the $\Delta\rho = 0$ position. For points III and IV the energy released is greater than the energy for pushing to depth. In the case with $\Theta_{bottom} = 2.4884\,^{\circ}C$ the interface between the two water masses is marginally stable and a small perturbation will release the potential energy. (b) Maximum energy released for the continuous warming of the bottom water in Fig. 6a with points highlighting the five water columns. There is a net energy release into the system.

column. We have only considered the energy released by changing the vertical positions of water parcels, or in a sense, overturning the water column. In either case, water parcel rearrangement or actual water mass mixing, the end result will be to move salty waters from the bottom of the ocean to the surface, or in low latitudes at least up to the base of the thermocline. The case of continuous stratification has been treated, leading to qualitatively similar results (not shown, see (Ingersoll, 2005) for the case of a simplified equation of state).

4. Discussion

4.1. Energetics and time scales

For a water column that is 4000 dbar deep (two layers, each 2000 dbars thick) our calculation indicates that about 0.16 J/kg of energy can be released into the water column by thermobaricity. In our 4000 dbar water column this corresponds to ~640,000 J/m^2. While 0.16 J/kg of energy might at first seem small, the fact that it applies over the whole water column leads to a large amount of energy released. Conversion of the 0.16 J/kg of potential energy into kinetic energy, if it is 100% efficient, corresponds to a root mean squared velocity of 0.57 m/s over the whole water column, which is very large relative to measured vertical motions in the modern ocean. In general, the energy/unit mass scales with the pressure squared and the total column energy scales with the pressure cubed (Akitomo, 1999a; Ingersoll, 2005). This strong dependence on depth is one of the main reasons our mechanism, which considers the whole deep ocean water column, generates so much energy. Studies of thermobaric instabilities in the modern ocean, generated by fresh water extraction from shallow mixed layers with small temperature inversions below them, find much lower total energy releases into the system (Killworth, 1979; Denbo and Skyllingstad, 1996). Thermobaric energy release should also be compared with the other sources of mechanical work in the ocean, the winds and the tides (Wunsch, 1998) (Table 1). As the thermobaric energy release does not have an inherent timescale, we convert the modern terms normally given in W/m^2 into an equivalent time scale to match the thermobaric energy. Approximately 2 years of either global wind or tidal work/unit area on the ocean is required to match our calculated energy release.

So, if the conditional instability can be triggered, there is a large amount of available potential energy that could be converted, virtually instantaneously, to kinetic energy. This sudden release is possible in our simple calculation because of the strong salinity gradient between the two water masses. Initially the water column is neutrally stable within each of the two layers,

Table 1

Work terms			Equivalent time
Energy source	Global (10^{12} W)	Area average (mW/m^2)	4000 dbar water column (years)
Wind	0.88	2.4	2.0
Tides	0.9	2.5	2.1

they are considered to be two well-mixed boxes, and it is very stable at the interface. This stability erodes as geothermal heat warms the deep water mass and the capacitor builds up until the entire water column is neutrally stable just at the point that the most energy has been stored in the system. At this point a small perturbation can easily trigger a finite amplitude instability, as any movement of water from the layer above into the layer below, via breaking internal waves for example, will cause the system to reorganize. The capacitor can be discharged before reaching the neutral stability condition at the interface if a large enough external perturbation is applied to move upper layer water parcels below the level of free convection (Garwood et al., 1994). The threshold for how much "noise" in the system is required to move water across the two-layer interface scales inversely with the degree to which the capacitor has charged. In other words, the capacitor can be discharged when the water column is stable if a large enough perturbation is added into the static column, or it can be activated by normal convection when the water column becomes slightly unstable at the layer interface. In this latter case, thermobaric convection strongly intensifies ordinary convection. At this point, the thermobaric energy can be released, virtually instantaneously, causing abrupt vertical overturning, as shown in numerical experiments of a two-layer ocean cooled at the top (Akitomo, 1999b).

But can geothermal heating provide the energy that a vertical salinity gradient allows there to be stored in the deep ocean? Is the geothermal source of comparable size to other heating and cooling terms in the system? Outside of a small region of the North Atlantic, water warmed by the heat flux at the bottom of the ocean lies on isopycnals that outcrop in the Southern Ocean. Annually averaged over the poles where this deep water is formed, the net heat release to the atmosphere is $\sim$100 W/m^2, about 10^3 times larger than geothermal input on a per unit area basis (Peixoto and Oort, 1992). However, the geothermal term operates over a much larger area than the polar heat exchange fluxes. In the MIT model, the area of heating from below is $10\times$ larger than the area where abyssal isopycnals outcrop. So, the input of 50 mW/m^2 at the bottom of the ocean is focused into a maximum heat loss of $\sim$700 mW/m^2 at the Southern Ocean surface (Adcroft et al., 2001). Due to spatial resolution problems in all GCMs, the real modern ocean has a much smaller area of deep-water formation in the Southern Ocean and focuses geothermal input to an even larger degree than the model result. The area of the modern ocean is $\sim 350\times10^6$ km^2. The area of the Southern Ocean between 80–85°S (the region around Antarctica) is $\sim 0.4\times10^6$ km^2. This factor of $1000\times$ means that the focused geothermal heating of 50 mW/m^2 is locally of the same order as the total heat exchange at high southern latitudes. The focusing effect of geothermal heating can cause this heat flux to be a significant fraction of the total heat loss in the crucial deep-water formation zones in the glacial Southern Ocean. This suggests that the geothermal heat is potentially relevant for determining the heat content of the abyssal waters.

Given that there is enough energy available to overturn the water column, we need to understand the inherent time scale to charge the capacitor. It will take about 10,000 years to heat 2 km of seawater by 2 °C with a 50 mW/m^2 heat flux (from a temperature close to the freezing point to a temperature at which the thermobaric capacitor is nearly fully charged, for a salinity difference of 0.4 psu). This implies that geothermal heating and the thermobaric effect together provide a mechanism that should be accounted for when studying climatic variations on several thousand-year time scales, e.g. Bond Cycles. There is an important caveat to this statement. Our calculation assumes the bottom water is stagnant, which is almost certainly not the case in the real glacial ocean. In fact, the rate of charging the thermobaric capacitor by geothermal heating will scale inversely with the overturning strength of the deep-sea. More sluggish circulation states will charge up the thermobaric capacitor faster than vigorous overturning. This 10,000-year number is also for a fully charged capacitor. There might be scenarios where shorter events, e.g. D/O Events, could be affected by thermobaricity if the relevant water mass was thinner or the required temperature difference was smaller.

The thermobaric capacitor has enough energy to overturn the water column, can be triggered by regular oceanic processes, and charges over a time scale that is relevant to the climate record. However, can the capacitor charge and then catastrophically release without just "leaking" away its energy first? Diapycnal mixing must be weak enough to keep the warm salty water below from slowly mixing with the cold fresh water above. The system has leaked away its energy if diapycnal mixing erases the temperature gradient between the upper and lower boxes. At steady state this temperature difference is set by the geothermal heat flux and the size of the diapycnal mixing coefficient:

$$\frac{\rho C k_v}{H}\left(\Theta_{top}-\Theta_{bottom}\right) = \text{geothermal flux}.$$

With appropriate numbers for the ocean (the geothermal flux is 50 mW/m^2, the heat capacity, C, is 4000 J/°C/kg, the density is 1000 kg/m^3 and the layer height, H, is 2000 m) and a vertical diffusivity of 10^{-4} m^2/s, Θ_{top}–$\Theta_{bottom,}$ $\Delta\Theta$, is 0.25 °C. This is about 10% of the fully charged capacitor we calculate for a salinity difference of 0.4 psu. Yet the modern mean vertical diffusivity of 1 cm^2/s needed to balance a whole overturning rate of ~20 Sverdrups is 10 × higher than most of the observations from the open ocean thermocline (Ledwell et al., 1993). Recent work has shown that there are large gradients in the spatial distribution of vertical mixing in the ocean (Polzin et al., 1997) with the highest values found near the coasts and over rough topography (Polzin et al., 1996; Ledwell et al., 2000; Heywood et al., 2002). Most of the deep open ocean diffusivity values are 0.1 cm^2/s or lower. In this case the $\Delta\Theta$ for our two boxes is 2.5 °C, a fully charged capacitor. This high degree of spatial variability was probably also the case in the glacial ocean and would allow the thermobaric capacitor to charge over large space scales without leaking away.

In addition to diapycnal mixing we must consider the effects of isopycnal mixing and its associated loss of heat at the outcrop region. This heat loss does not work to erase the capacitor because it does not warm the cold and fresh upper layer. Isopycnal mixing does not "leak" away the energy before it can charge a capacitor, but it can reduce the total amount of heat in the deep layer by radiating the geothermal flux to the atmosphere at the deep-water outcrop region. If the capacitor is to charge from below, the total geothermal heat input must be larger than the *net* heat loss at the Antarctic air/sea interface. In the MIT model experiments a 50 mW/m^2 input at the bottom of the ocean warmed the deep water by 0.3° on average. This is only about 10% of the fully charged capacitor we calculated in the previous section. But as we discussed above, the amount of heating, and therefore the bottom water temperature increase is set by the ratio of the heating area to the isopycnal outcrop area. The MIT model's ratio of ~10 is at least a factor of 10 too small for the real ocean and a bottom water temperature increase of a few degrees is clearly within reason. Further model studies are required to quantify this effect, but the isopycnal "leak" may not be large.

4.2. Consistency with paleo data

Thermobaric capacitance in the glacial deep ocean provides a plausible mechanism to explain the series of events within with a Bond Cycle and its associated early warming in Antarctica (Fig. 1). D/O events in the Greenland ice core are initiated by an abrupt warming (δ^{18}O increase), followed by a gradual cooling (over a few hundred to a few thousand years), and then are terminated by a cooling that is nearly as abrupt as the original warming (δ^{18}O decrease). While these events may also represent capacitance in the deep ocean system, our calculation of the time needed for a full thermobaric charge-up is too long to explain them. However, D/O events are further grouped into so called "Bond Cycles" (Bond et al., 1993). Following a Heinrich event there is an especially large warming (e.g. D/O #'s 8, 12 and17) in the Greenland record that is followed by a series of progressively smaller amplitude D/O events until the next Heinrich event terminates the cycle (Fig. 1). In the Antarctic records the abrupt warmings are a more gradual trend that starts 1–3000 years before the large warming in the Greenland record, and that begins cooling again at the same time the north warms (Blunier and Brook, 2001) (see "Greenland Pattern" and "Antarctic Pattern" in Fig. 1). This different response of the north and south is the classic "bi-polar see-saw" (Broecker, 1998) and has a plausible explanation in thermobaricity.

Early warming around Antarctica, thousands of years before the rapid warming seen in Greenland, could be the natural result of heating the deep isopycnals that outcrop in the Southern Ocean. As was observed in modern GCM runs (Adcroft et al., 2001), a global input of 50 mW/m^2 will be focused at the relatively restricted area of the Antarctic surface and will lead to large surface heat fluxes. This focusing of the global geothermal input occurs because, outside of the North Atlantic, abyssal isopycnals outcrop in the Southern Ocean. In our scenario, the early warming of Antarctic ice cores means that some of the geothermal heat must be leaking out of the system, but it also means that enough heat remains in the deep to charge the thermobaric capacitor. Heating of the salty deep ocean stores energy in this layer until the critical depth for thermobaric convection shrinks to a point where it can be triggered by natural low amplitude oceanic processes (Garwood et al., 1994), or "normal" convection itself.

This catastrophic overturning event brings warm salty water to the surface, or near surface layers, and could provide a negative freshwater forcing to "kick start" overturning in the high latitude north, and therefore cause the observed rapid warming in the Greenland records. In a sensitivity study of the overturning circulation under glacial boundary conditions (Ganopolski and Rahmstorf, 2001), an increase in evaporation minus precipitation in the high latitude North Atlantic was enough to switch the northern overturning circulation from an "off" mode to an "on" mode. Here we propose that this negative freshwater forcing could come from below, not from above. The LGM temperature and salinity diagram puts southern source cold/salty water in the bottom of the ocean. Something must change this water mass' buoyancy before salt forcing at the surface could create a dense enough water mass to initiate a new mode of

overturning. Geothermal heating can provide the needed buoyancy to the deep waters and thus decrease the surface to deep density difference. In addition, the thermobaric effect itself can provide the needed abrupt salt pulse from below by mixing salty water stored in the deep into the shallow ocean. This re-start of northern sinking leads to rapid warming of the atmosphere, as recorded in the Greenland ice core, and simultaneous cooling of the Southern Hemisphere due to the classic "see-saw" effect (Fig. 1), where heat is extracted from the south by deep water formation in the north (Broecker, 1998). In our scenario, Bond Cycles still end with a Heinrich event and the massive fresh water forcing is enough to stall the northern source overturning, just as in the previous models.

This proposed mechanism makes an important prediction. The deep ocean should be warming while the climate system above is deteriorating through a Bond Cycle. In fact, two other pieces of the paleoclimate record are consistent with deep-ocean warming during a Bond Cycle. Fig. 1C shows the benthic $\delta^{18}O$ record from core MD95-2042 from 3500 m off the coast of Portugal (Shackleton et al., 2000). There are several benthic $\delta^{18}O$ decreases that are due to a combination of deep-ocean warming and/or a decrease in global ice volume (because glacial melt waters decrease the ocean $\delta^{18}O$). We must consider the effect of ice volume variations on the water $\delta^{18}O$ because, within the errors of the MD95-2042 age model, the lighter benthic foraminifera are roughly synchronous with the Heinrich melting. In a recent paper, Chappell has used the shape of stage 3 coral terraces from the Huon Peninsula to constrain the shape of relative sea level change from 65 to 20 ka (Chappell, 2002) and therefore the amount of melt water that entered the ocean during rapid sea level rise. Accounting for these results, Chappell calculated the residual $\delta^{18}O_{benthic}$ in MD95-2042 that must be due to deep-ocean warming for each of the light benthic events. These are the black numbers in Fig. 1C. From this evidence, though we still do not know exactly when it happened, the deep ocean could have warmed by ~0.5–2.0 °C while climate was deteriorating prior to the end of Heinrich events and the large D/O warming. In addition, the benthic $\delta^{13}C$ record in this same core shows very light values at this time, consistent with more sluggish deep circulation, where it is easier to charge the capacitor. These very light $\delta^{13}C$ values have also been found in the tropical deep Atlantic (Curry and Oppo, 1997). Both of these observations are consistent with the thermobaric effect and geothermal heating leading to some of the rapid climate changes seen in the ice core.

One problem with this analysis of the data is that the records are also consistent with the bi-polar see–saw hypothesis. During the largest Greenland stadials and Heinrich events, a hypothesized reduction in the flux of northern source waters would also lead to Antarctic and deep ocean warming. However, in the thermobaric capacitor idea this warming should be confined to salty bottom waters, whereas in the see–saw there should be warming in much of the water column. If we could collect depth profiles of temperature during these key climatic extremes, we should be able to distinguish between the two ideas. Relatively shallow benthic $\delta^{18}O$ and Mg/Ca records are an important test of our idea.

The steady state imprint of geothermal heating at the LGM can be seen in Fig. 7. It has been known for many years that there is a global trend in the absolute value of $\delta^{18}O$ in benthic foraminifera from the LGM. The North Atlantic foraminifera are about 0.5‰ heavier than the Pacific ones. This difference must be due to a combination of warmer and/or isotopically lighter waters in the glacial Pacific relative to the glacial Atlantic. In the past it has not been possible to separate these two effects, but we now know from pore fluid data that the LGM North Atlantic water was isotopically *lighter* than the rest of the ocean (Adkins et al., 2002). Therefore, the 0.5‰ decrease in benthic foraminifera from the Atlantic to the Pacific must be due to at least a 2 °C warming along this water mass trajectory. While this is similar to the amount of warming needed to charge our LGM thermobaric capacitor, the point here is that a global compilation of benthic $\delta^{18}O$ data implies that geothermal heating was significantly warming the glacial ocean. The same effect is seen in models of the modern circulation because the abyssal isopycnals in the Pacific are less well ventilated and spend a longer time next to the geothermal heat source (Adcroft et al., 2001). It is important to note that a warmer glacial Pacific does not mean the Atlantic had more Sverdrups of deep-water formation. Just from its ~3 times larger size, the Indo-Pacific basin will have older ventilation ages, and warmer water, than the Atlantic if we assume the same flux of southern source deep water to both the Atlantic and the Indo/Pacific.

If the thermobaric effect and the geothermal heat flux are behind some of the large amplitude climate shifts seen during the last glacial period, they also provide an explanation for why there have been no large amplitude events during the Holocene (Grootes et al., 1993). Salinity stratification is crucial for warm water to be stored in the deep ocean and then catastrophically released. From pore fluid data we know that somewhere between the LGM and today the deep stratification switched from haline domination to thermal domination. If the Holocene has the same deep water T/S arrangement as the modern ocean, it cannot support the accumulation of warm/salty deep waters that leads to thermobaric convection from below.

We have identified three features of the glacial deep ocean that could combine to cause some of the observed rapid climate changes. The first two, thermobaricity and

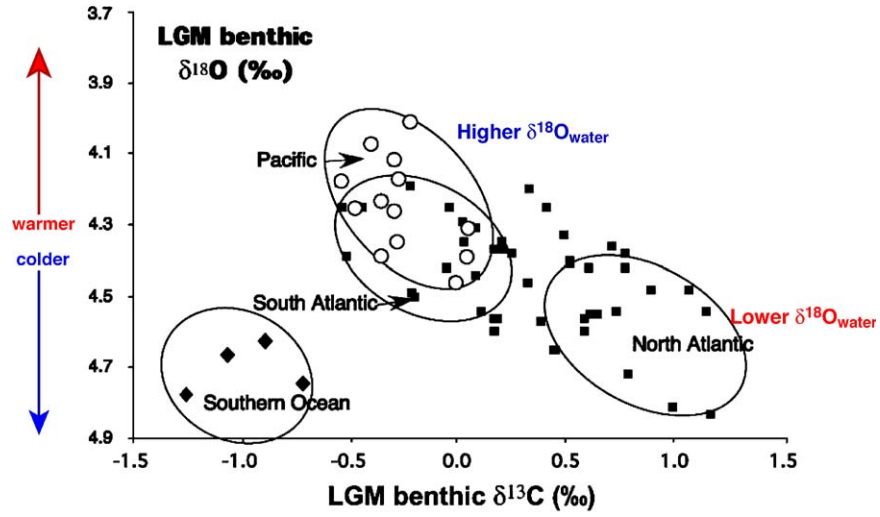

Fig. 7. Summary of benthic foraminifera and water $\delta^{18}O$ stable isotope data from the LGM (adapted from Duplessy et al., 2002). Coupled with the pore water data that shows lighter $\delta^{18}O$ values for the water in the glacial Atlantic than in the glacial Southern Ocean and Pacific, this compilation implies that the abyssal Pacific contained the warmest waters at the LGM. This pattern is consistent with geothermal heating warming the deep ocean by at least 2 °C.

geothermal heating, are independent of climate state. The third, deep stratification due to salt gradients is found during the LGM, and by inference during isotopic stages 3 and 4, but not during the Holocene. However, we have not proven that a thermobaric capacitor did indeed exist in the past ocean. We have only shown that geothermal heat and the seawater equation of state are a possible heat source and energy storage mechanism that might be part of the explanation for rapid climate changes during the last glacial period. The key weakness in our argument is the unknown "leakiness" of the system to heat input at the bottom. This erosion of the density contrast between upper and lower waters will also affect the unknown spatial extent of where the capacitor will build up. If diapycnal mixing can remove the warm and salty versus cold and fresh gradient in the deep ocean faster than the capacitor can charge and release, our mechanism of salt water forcing from below did not cause the abrupt warmings seen in the record. An important next test is to include thermobaricity and geothermal heating in a hierarchy of models from a simple "Stommel" box model of the overturning circulation, to a basin scale 2-D model, to an ocean GCM where salty deep waters are produced in the Southern Ocean. Future data collection about the location and strength of salinity stratification in the glacial deep ocean would also help constrain the area over which a thermobaric capacitor might charge. Finally, radiocarbon data from the past ocean could constrain the rate of deep overturning through time and indicate periods where a thermobaric capacitor might be more likely to charge up.

5. Conclusion

There are several aspects of the last glacial cycles that require storage of energy in the climate system; deglaciations, D/O events, and Bond Cycles. Two aspects of the glacial deep ocean motivate us to suggest a mechanism that could provide the energy storage, and its rapid release, required to explain the record of abrupt climate change. First, pore water data indicate that the glacial deep ocean was dominated by salinity, as opposed to thermal, stratification. Second, benthic foram $\delta^{18}O$ data from the LGM, when combined with pore fluid estimates of the distribution of water $\delta^{18}O$ at the LGM, show that the deep Pacific was warmer than the deep North Atlantic by ~2 °C. In the presence of a salt stratified deep ocean, geothermal energy can warm the deepest layers of the ocean while maintaining the static stability of the water column. The coupled dependence of seawater density on temperature and pressure (thermobaricity) allows for a virtually instantaneous release of the energy stored in the warm deep water, causing abrupt overturning of the water column. This overturning can bring salt to the areas of deep-water convection in the glacial North Atlantic and potentially induce a reinvigoration of northern source deep-water formation. The hypothesized scenario provides an independent mechanism for fueling the "NADW on" phase of an Atlantic salt oscillator while geothermal heat reduces the buoyancy of the very dense, salty and cold, deep waters found during the LGM. Estimates of the diapycnal diffusivity in the Glacial Ocean and results from Ocean

GCMs will be extremely useful to verify that the energy storage mechanism described in this paper could have actually taken place.

Acknowledgements

Early discussions with M. Bender, D. Sigman and T. Schneider helped form our ideas. The manuscript was improved by thoughtful reviews from R. Toggweiller and S. Hostetler. JFA was supported by NSF grant OCE-0096814.

Appendix A1

This Appendix is devoted to the derivation of the amount of potential energy that can become available for conversion into kinetic energy by rearranging a stable water column, under the hypothesis that no mixing takes place. Considering that no work is done on the whole water column, energy conservation implies that the energy available for conversion into kinetic energy after the rearrangement corresponds to the variations of internal energy U and of gravitational potential energy G:

$$U_{\mathrm{in}} + G_{\mathrm{in}} = U_{\mathrm{fin}} + G_{\mathrm{fin}} + KE, \tag{A.1}$$

where subscripts *in* and *fin* refer to the initial and final state, respectively.

Consider first a parcel A of water of density ρ_{parcel} located at pressure p_{i} and exchange its position with a parcel of water of density ρ_{fluid} with the same mass located just below parcel A. The exchange occurs in adiabatic conditions and no mixing is allowed. When the adiabatic expansion of the rising parcel does not balance the adiabatic compression of the falling parcel A, there will be a net volume change. This occurs when the two parcels have different temperatures, since the adiabatic compressibility of seawater depends on temperature. This is the thermobaric effect. Because there is a volume change, the two-parcel system does work on its surroundings. The first law of thermodynamics ensures that the work is balanced by a change in internal energy. This work goes into the water column above, which is lifted (or lowered) according to the expansion (or compression) of the two-parcel system. The vertical movement of the upper column occurs in adiabatic and isobaric conditions. The work is entirely converted into gravitational potential energy of the upper column; its internal energy does not change.

Using subscripts p and u for the two-parcel system and the upper column respectively, we expand the gravitational potential energy in Eq. (A.1) into its two components:

$$U_{\mathrm{in,p}} + G_{\mathrm{in,p}} + G_{\mathrm{in,u}} = U_{\mathrm{fin,p}} + G_{\mathrm{fin,p}} + G_{\mathrm{fin,u}} + KE. \tag{A.2}$$

The above discussion indicates that the change of internal energy in the two-parcel system is compensated by the variation in gravitational potential energy of the upper column, and no other changes in internal energy occur in the system:

$$U_{\mathrm{in,p}} + G_{\mathrm{in,u}} = U_{\mathrm{fin,p}} + G_{\mathrm{fin,u}}. \tag{A.3}$$

Insertion of Eq. (A.3) into Eq. (A.2) leads to

$$G_{\mathrm{in,p}} = G_{\mathrm{fin,p}} + KE. \tag{A.4}$$

The latter equation indicates that the potential energy available for conversion into kinetic energy after the switch in the position of the two parcels corresponds to the variation in the gravitational potential energy of the two-parcel system only, and not to that of the whole column. As pointed out by Reid et al. (1981) and Mcdougall (2003), the gravitational potential energy change of the whole column is different from the total energy change (internal plus gravitational), because the fluid is thermobaric.

Two contributions enter into the variation of gravitational potential energy of the two switching parcels: the decrease of G associated with lowering parcel A by the vertical size of the fluid parcel ($\mathrm{d}z_{\mathrm{fluid}}$), and the increase of G associated with raising the fluid parcel by the vertical size of parcel A ($\mathrm{d}z_{\mathrm{parcel}}$). Using the hydrostatic equation $\mathrm{d}p = \rho g\,\mathrm{d}z$, and remembering that the two parcels have the same mass (such that the pressure difference $\mathrm{d}p$ between the bottom and top of each parcel is the same), we can write $\mathrm{d}z_{\mathrm{fluid}} = 1/(\rho_{\mathrm{fluid}} g)\ \mathrm{d}p$ and $\mathrm{d}z_{\mathrm{parcel}} = 1/(\rho_{\mathrm{parcel}} g)\ \mathrm{d}p$. The decrease of gravitational potential energy per unit mass corresponding to the exchange between the positions of the two parcels is therefore $[g(\mathrm{d}z_{\mathrm{fluid}} - \mathrm{d}z_{\mathrm{parcel}})] = (V_{\mathrm{fluid}} - V_{\mathrm{parcel}})\mathrm{d}p$, where V_{parcel} and V_{fluid} are the specific volumes of the two parcels computed at pressure p_{i} and $\mathrm{d}p$ is the increase in pressure experienced by parcel A.

We now repeat the process of switching position between parcel A and the fluid parcel located just below it, until parcel A reaches the pressure p_{f}. The total variation of potential energy per unit mass is

$$KE/m = \int_{p_{\mathrm{i}}}^{p_{\mathrm{f}}} (V_{\mathrm{fluid}} - V_{\mathrm{parcel}})\,\mathrm{d}p. \tag{A.5}$$

If the parcel is moved from pressure $p_{\mathrm{i}} = p'$ to pressure $p_{\mathrm{f}} = p' + p_{\mathrm{m}}$ as in the experiment described in the text, Eq. (1) is recovered.

When all the water initially located between pressures $p_{\mathrm{i}} - \Delta p$ and p_{i} is moved to the pressures between $p_{\mathrm{f}} - \Delta p$ and p_{f}, the total kinetic energy released per unit mass of

the displaced water is

$$\frac{KE(\Delta p)}{m} = \frac{1}{\Delta p} \int_{p_i - \Delta p}^{p_i} \mathrm{d}p' \left[\int_{p'}^{p' + p_f - p_i} (V_{\mathrm{fluid}} - V_{\mathrm{parcel}})\, \mathrm{d}p \right]. \tag{A.6}$$

Eq. (2) is recovered when $p_i = p_m$, $p_f = p_b$ and the energy is divided by the total mass of the water column, instead of the mass of displaced water.

References

Adcroft, A.A., Scott, J.R., Marotzke, J., 2001. Impact of geothermal heating on the global ocean circulation. Geophysical Research Letters 28, 1735–1738.

Adkins, J.F., McIntyre, K., Schrag, D.P., 2002. The salinity, temperature, and $\delta^{18}O$ of the glacial deep ocean. Science 298, 1769–1773.

Akitomo, K., 1999a. Open-ocean deep convection due to thermobaricity 1. Scaling argument. Journal of Geophysical Reaserch 104, 5225–5234.

Akitomo, K., 1999b. Open-ocean deep convection due to thermobaricity 2. Numerical experiments. Journal of Geophysical Reaserch 104, 5235–5249.

Behl, R.J., Kennett, J.P., 1996. Brief interstadial events in the Santa Barbara basin, NE Pacific, during the past 60 kyr. Nature 379, 243–246.

Blunier, T., Brook, E., 2001. Timing of millennial-scale climate change in Antarctica and Greenland during the last glacial period. Science 291, 109–112.

Bond, G., Broecker, W.S., Johnsen, S., McManus, J., Labeyrie, L., Jouzel, J., Bonani, G., 1993. Correlations between climate records from North Atlantic sediments and Greenland ice. Nature 365, 143–147.

Boyle, E.A., Keigwin, L.D., 1987. North Atlantic thermohaline circulation during the last 20,000 years linked to high latitude surface temperature. Nature 330, 35–40.

Broecker, W.S., 1998. Paleocean circulation during the lst deglaciation: a bipolar seasaw? Paleoceanography 13, 119–121.

Broecker, W.S., Bond, G., Klas, M., Bonani, G., Wolfli, W., 1990. A salt oscillator in the glacial northern Atlantic? 1. The concept. Paleoceanography 5, 469–477.

Chappell, J., 2002. Sea level changes forced ice breakouts in the Last Glacial cycle: new results from coral terraces. Quaternary Science Reviews 21, 1229–1240.

Charles, C.D., Lynch-Stieglitz, J., Ninnemann, U.S., Fairbanks, R.G., 1996. Climate connections between the hemisphere revealed by deep sea sediment core/ice core correlations. Earth and Planetary Science Letters 142, 19–27.

Curry, W.B., Oppo, D.W., 1997. Synchronous, high-frequency oscillations in tropical sea surface temperatures and North Atlantic Deep Water production during the last glacial cycle. Paleoceanography 12, 1–14.

Denbo, D.W., Skyllingstad, E.D., 1996. An ocean large-eddy simulation model with application to deep convection in the Greenland Sea. Journal of Geophysical Reaserch 101, 1095–1110.

Duplessy, J.-C., Labeyrie, L., Waelbroeck, C., 2002. Constraints on the ocean oxygen isotopic enrichment between the Last Glacial Maximum and the Holocene: paleoceanographic implications. Quaternary Science Reviews 21, 315–330.

Duplessy, J.C., Shackleton, N.J., Fairbanks, R.G., Labeyrie, L., Oppo, D., Kallel, N., 1988. Deep water source variations during the last climatic cycle and their impact on the global deep water circulation. Paleoceanography 3, 343–360.

Dutay, J.-C., Madec, G., Iudicone, D., Jeanbaptiste, P., Rodgers, K., 2004. Study of the impact of the geothermal heating on ORCA model deep circulation deduced from natural helium-3 simulations. Geophysical Research Abstracts 6 1607-7962/gra/EGU04-A-02530.

Fofonoff, N.P., 1985. Physical properties of seawater: a new salinity scale and equation of state of seawater. Journal of Geophysical Reaserch 90, 3332–3342.

Ganopolski, A., Rahmstorf, S., 2001. Rapid changes of glacial climate simulated in a coupled climate model. Nature 409, 153–158.

Garwood, R.W., Isakari, S.M., Gallacher, P.C., 1994. Thermobaric convection. In: Johannesen, O. M., Muench, R. D., Overland, J. E. (Eds.), The Polar Oceans and their Role in Shaping the Global Environment. Geophysical Monograph Series, Vol. 85. American Geophysical Union, Washington, DC, pp. 199–209.

GRIP, 1993. Climate instability during the last interglacial period recorded in the GRIP ice core. Nature 364, 203–207.

Grootes, P.M., Stuiver, M., White, J.W.C., Johnsen, S., Jouzel, J., 1993. Comparison of oxygen isotope records from GISP2 and GRIP Greenland ice cores. Nature 366, 552–554.

Hays, J.D., Imbrie, J., Shackleton, N.J., 1976. Variations in the earth's orbit: pacemaker of the ice ages. Science 194, 1121–1132.

Heinrich, H., 1988. Origin and consequences of cyclic ice rafting in the northeast Atlantic Ocean during the past 130,000 years. Quaternary Research 29, 142–152.

Hemming, S.R., 2004. Heinrich events: massive late Pleistocene detritus layers of the North Atlantic and their global climate imprint. Reviews of Geophysics 42, RG1005.

Heywood, K.J., Naveria-Garabato, A.C., Stevens, D.P., 2002. High mixing rates in the abyssal Southern Ocean. Nature 415, 1011–1014.

Huang, R.X., 1999. Mixing and energetics of the oceanic thermohaline circulation. Journal of Physical Oceanography 29, 727–746.

Hughen, K.A., Overpeck, J.T., Peterson, L.C., Trumbore, S., 1996. Rapid climate changes in the tropical Atlantic region during the last deglaciation. Nature 380, 51–54.

Ingersoll, A.P., 2005. Boussinesq and an elastic approximation revisited: application to thermobaric instability. Journal of Physical Oceanography in press.

Keeling, R.F., Stephens, B.B., 2001. Antarctic sea ice and the control of Pleistocene climate instability. Paleoceanography 16, 112–131.

Killworth, P.D., 1979. On "chimney" formation in the ocean. Journal of Physical Oceanography 9, 531–554.

Labeyrie, L.D., Duplessy, J.-C., Duprat, J., Juilet-Leclerc, A., Moues, J., Michel, E., Kallel, N., Shackleton, N.J., 1992. Changes in the vertical structure of the North Atlantic Ocean between glacial and modern times. Quaternary Science Reviews 11, 401–413.

Ledwell, J.R., Montgomery, E.T., Polzin, K.L., St. Laurent, L.C., Schmitt, R.W., Toole, J.M., 2000. Evidence for enhanced mixing over rough topography in the abyssal ocean. Nature 403, 179–182.

Ledwell, J.R., Watson, A.J., Law, C.S., 1993. Evidence for slow mixing across the pycnocline from an open-ocean tracer-release experiment. Nature 364, 701–703.

McDougall, T., 2003. Potential enthalpy: a conservative oceanic variable for evaluating heat content and heat fluxes. Journal of Physical Oceanography 33, 945–963.

McDougall, T.J., 1987. Thermobaricity, cabbeling, and water-mass conversion. Journal of Geophysical Research 92, 5448–5464.

Peixoto, J.P., Oort, A.H., 1992. Physics of Climate. American Institue of Physics.

Polzin, K.L., Speer, K.G., Toole, J.M., Schmitt, R.W., 1996. Intense mixing of Antartic Bottom Water in the equatorial Atlantic Ocean. Nature 380, 54–57.

Polzin, K.L., Toole, J.M., Ledwell, J.R., Schmitt, R.W., 1997. Spatial variability of turbulent mixing in the abyssal ocean. Science 276, 93–96.

Reid, J., Elliot, B.A., Olsen, D.B., 1981. Available potential energy: a clarification. Journal of Physical Oceanography 11, 15–29.

Schulz, H., von Rad, U., Erlenkeuser, H., 1998. Correlation between Arabian Sea and Geenland climate oscillations of the past 110,000 years. Nature 393, 54–57.

Scott, J.R., Marotzke, J., Adcroft, A.A., 2001. Geothermal heating and its influence on the meridional overturning circulation. Journal of Geophysical Reaserch 106, 31141–31154.

Shackleton, N.J., Hall, M.A., Vincent, E., 2000. Phase relationships between millennial-scale events 64,000–24,000 years ago. Paleoceanography 15, 565–569.

Stein, C.A., Stein, S., 1992. A model for the global variation in oceanic depth and heat flow with Lithospheric age. Nature 359, 123–129.

Stocker, T.F., Johnsen, S.J., 2003. A minimum thermodynamic model for the bipolar seesaw. Paleoceanography 18 (4), 1087.

Wunsch, C., 1998. The work done by the wind on the oceanic general circulation. Journal of Physical Oceanography 28, 2332–2340.

Wunsch, C., Ferrari, R., 2004. Vertical mixing, energy and the general circulation of the oceans. Annual Review of Fluid Mechanics 36, 281–314.